communications engineering

A Nature Portfolio journal

Article

https://doi.org/10.1038/s44172-025-00405-6

Electro-quasistatic and resonant cavity car body communication

Check for updates

David Yang & Shreyas Sen

Wired protocols such as Controller Area Network (CAN) dominate in-vehicle communication today. While reliable, these protocols entail intricate installation procedures. Recent advancements in communication technologies utilizing Electro-Quasistatic Fields (EQS) through conductors have ushered in alternative communication techniques. This work introduces EQS car body communication, recognizing the potential of the car's chassis as a medium to confine EQS fields. This alternative approach offers a new modality for efficient intra-vehicle wireless communication, addressing power efficiency and physical security concerns. Furthermore, this research demonstrates that a vehicle can be treated as a resonant cavity, providing low-loss, wideband channels for high-speed communication. Theoretical analysis, electromagnetic simulations, and measurements conducted in a consumer-grade vehicle highlight the viability of these new intra-vehicle communication techniques. This fundamentally new approach utilizes different physical modalities, harnessing the car medium itself and opening doors to modalities that have the potential to augment or even replace existing communication in automotive systems.

In-vehicle networks today primarily utilize twisted pair conductors such as controller area network (CAN)[1] to communicate between the vehicle's various electronic control units (ECUs) (Fig. 1a). With automotive features increasing exponentially in number and the continuous demand for smaller form factor vehicles, wire harnesses pose a considerable challenge both from a logistical and packaging perspective. The usage of return path wires and conductors in order to realize grounding in electronic communication first arose in telegraphy in the mid-nineteenth century. At the time, Maxwell equations, electromagnetic (EM) wave physics, and advanced circuit theory were in their infancy or not yet fully distilled. Later in the twentieth century, the invention of radio communication and decades of Moore's law scaling and research have led to reliable radiative wireless systems that have permeated all aspects of life. Past research on intra-vehicle communication security and other papers that survey in-vehicle networks have discussed wireless in-vehicle networks as a possibility, such as the survey of technology and trends by Tuohy et al.[2], Lu et al.[3], and Zeng et al.[4] However, significant drawbacks are present in wireless in-vehicle networks presented thus far. Reliability concerns directly arise from data loss due to high and variable channel losses of radiative communication systems[5,6]. In addition, concerns of remote hacking due to use of wireless network is prevalent[7–9]. The security vulnerability primarily arises from the radiative and isotropic nature of antennas in conventional radio communication systems (such as Bluetooth, Wi-fi, etc.). Wireless signals will continue to travel through the air without discrimination for intended receivers (Fig. 1a).

Though encryption presents a valid solution to prevent remote tampering, the elimination of external access to the signals from a physical layer prevents any sort of attack or exploitation of vulnerabilities that exist in the mathematical security employed. Intra-vehicle automotive systems today do not employ encryption due to the low probability of remote attack while the vehicle is in motion, as the wires tend to be embedded deeper within the automotive chassis. In the proposed technique, the physical layer would eliminate or greatly reduce access to the signals from outside or off the vehicle body, shifting the physical layer closer to the existing CAN system in place today while retaining the benefits of being wireless.

Traditional wired mediums including technologies that have received adoption or interest include LIN[10], FlexRay[11], MOST[12], and most recently Ethernet[13]. These technologies are both more energy efficient and robust as compared to wireless mediums but require a physical forward conducting and return path connection and hence can lead to increased packaging costs and overhead.

In this paper, the authors present modes of wireless communication that do not rely on radiation or necessitate return path conductors. The objective is to present a range of fundamentally new techniques supported by measurement data and numerical EM simulations. Ultimately, these modes have the potential to enhance or, in the distant future, even supplant traditional wired mediums with secure wireless alternatives and increase the amount of available space within a vehicle.

Department of Electrical and Computer Engineering, Purdue University, West Lafayette, IN, USA. e-mail: shreyas@purdue.edu

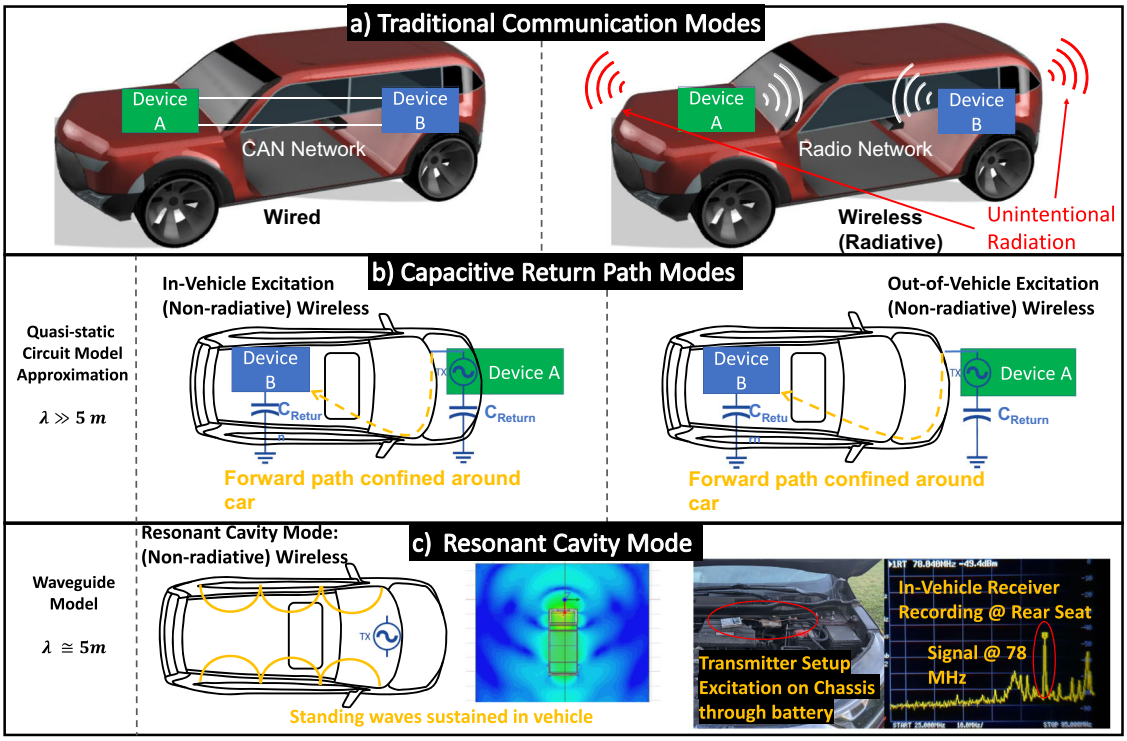

Fig. 1 | Comparison of various modes of intra-vehicular communication. a Highlights the existing communication modalities. **b** Application of previously proposed capacitive return path-based communication in intra-vehicle scenario. **c** Resonant cavity mode proposed by this paper.

Inspired by human body communication (HBC) theory, introduced by Zimmerman[14] and recent invention of electro-quasistatic (EQS) HBC, which leverages the conductive nature of the human body to communicate data in the near field—the same physics can be applied to the automotive car body. The later works that utilize EQS field-based body communication—enabled by a deeper understanding of the EQS body circuit model by Maity et al.[15] and return path capacitance[16] by Nath et al. coupled with a proposal of high impedance capacitive termination (patent by Sen and Maity)[17] led to EQS-HBC by Das et al.[18]. Since the vehicle itself is a large conductor and presents a large capacitance to the environment, a natural return path already exists[19,20]. Varga et al. also independently demonstrated groundless body communication devices, although not strictly EQS. Figure 1b highlights the path the signal takes through the vehicle from device A to device B and has a common reference through capacitive coupling of the devices' ground to the earth—commonly referred to as return path capacitances.

Das et al.[18] have also previously measured the signal confinement properties of using EQS communication. The additional confinement benefit compared to radiative technologies is significant in reducing any information from exiting the vehicle. Hence, the attack surface of EQS-based wireless systems is significantly improved over conventional radiative wireless.

This communication has the additional security benefits of the physically wired system, but achieves it wirelessly. For the first time in literature, this paper evaluates capacitive return-path techniques in an intra-vehicle application. To accomplish this, a study with both EM field simulations and in-vehicle measurements is presented. This paper also introduces a novel communication modality by exciting the car chassis as a rectangular cavity resonator. Simulations are performed in ANSYS high-frequency structure simulator (HFSS) in order to gain physical insight and numerical solutions of the communication channel. In addition, a microcontroller-based transmitter and custom receiver front-end with a commercially available spectrum analyzer setup are built to characterize channel loss and verify results. Section 2 covers the key results and discussion of the studies conducted on the proposed communication modes. Section 3 discusses the conclusion and implications of this research. Finally, Section 4 contains the methods and techniques employed in measurements and EM numerical analysis.

Results and discussion

Communication mode summary

No significant innovation in intra-vehicular communication physical layer has occurred in the past decade (Table 1) that is fundamentally different from traditional wired or wireless systems. Prior to the design and analysis of groundless wired systems (particularly advancements in HBC field for wearable devices) there were no suitable alternative physics that could replace wires yet retain wireline communication properties of security and reliability.

Table 1 breaks down the key differences between existing automotive communication networks and the proposed technique. This paper is focused primarily on the physical layer of communication. This work does not analyze Vehicle-to-Vehicle or Vehicle-to-Infrastructure, such as the works in Gerla and Kleinrock's review[21] or Kenney's work[22]. This paper primarily explores alternative wireless techniques to intra-vehicle networks that are currently implemented with CAN or variants of CAN like CAN-FD.

The table compares the operation bitrate evaluated from the channel loss derived numerical simulation and measurement. The third column considers the maximum range that is possible by each mode. As an example, the CAN signal can typically go as far as the twisted pair cable length inside the vehicle, whereas inside excitation, capacitive return path modes can at most communicate at about a meter. Furthermore, it examines the principal location of energy (or medium) for the communication system. Lastly, it evaluates the physical security of the communication method. Physical security is defined by evaluating the distance at which the electric field away from the vehicle chassis could be potentially intercepted or detected. For this metric, an electric field intensity floor of 10uV/m or below is considered.

Theoretical overview and physics of proposed modes

This section briefly underlines the theoretical physical setup that separates the various proposed physical modalities of communication.

Figure 2a highlights the excitation structure for an inside-excitation (asymmetric galvanic or bi-phasic) mode with signal conduction mechanisms like in the works of Chatterjee et al.[23]. A strong and localized current excitation exists at the transmitter because of the capacitive coupling

Table 1 | Key metric comparison of proposed modes versus existing modes

Technology	Operation bitrate	Max range	Communication medium	Detectable from Chassis (meters)
CAN	1 Mbps	Determined by cabling	Single twisted pair	0
LIN	19.2 kbps	Determined by cabling	Single forward path wire, common ground connection	0
FlexRay	20 Mbps	Determined by cabling	Single twisted pair, fiberoptic	0
MOST	150 Mbps	Determined by cabling	Fiberoptic	0
Ethernet	400 Gbps	Determined by cabling	4 twisted pairs, typically copper	0
Radiative wireless (Bluetooth, Wi-Fi, 900 MHz, mmWave)	Variable	Variable	Air or dielectric	>12
EQS inside excitation capacitive return path [this paper]	10 Mbps	1m	Surface	0 (Fig. 3c)
EQS outside excitation capacitive return path [this paper]	10 Mbps	Determined by length of chassis (~4 m)	Surface of vehicle chassis (no additional wires)	~1 (Fig. 4c)
Resonant cavity mode [this paper]	100 Mbps	Determined by perimeter of chassis (~2 or 4 m)	Air or dielectric inside chassis (no additional wires)	~1* (Fig. 4b)

Provides the key differentiation between the different communication modes.
*If voltage scaling techniques are employed to reduce the range of fields as in Fig. 4b.

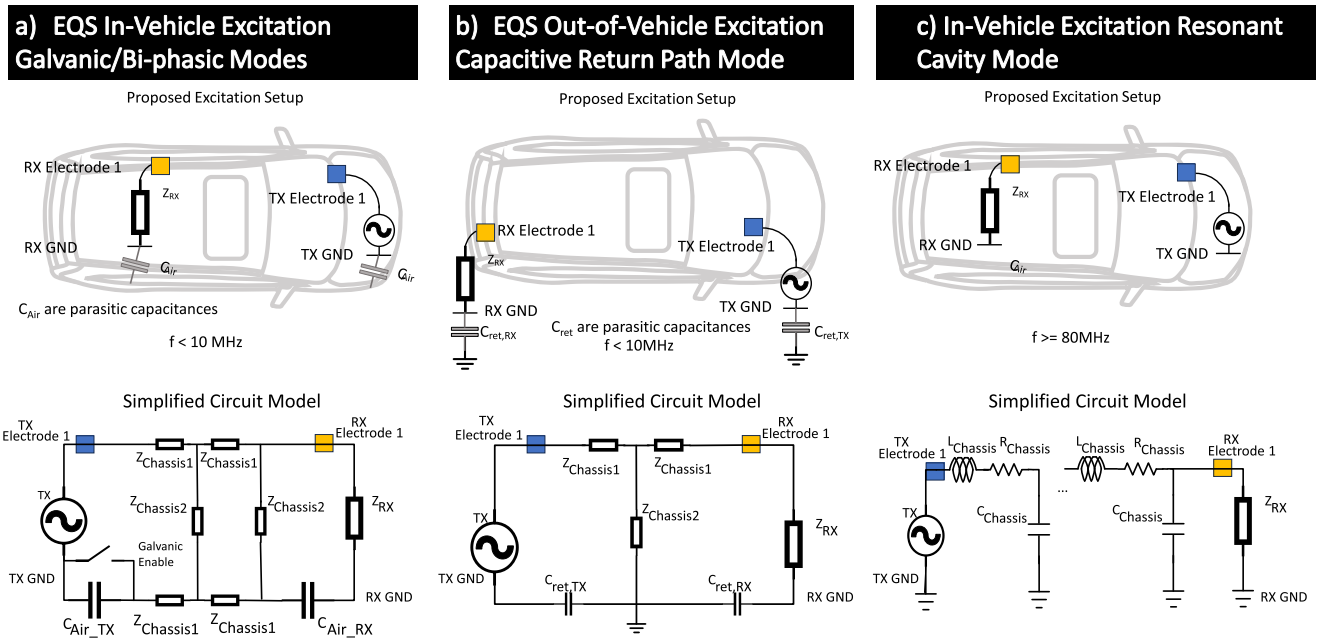

Fig. 2 | Theoretical diagram and circuit model. a Inside excitation (bi-phasic/galvanic) measurements. **b** Outside excitation (capacitive return path) channel measurements, and **c** resonant cavity mode measurements in the Electro-quasistatic (EQS) regime. Depictions include local transmitter (TX) and receiver (RX) ground (GND) references.

between the transmitter ground and the chassis ($C_{air,TX}$) that wraps around the device. The model becomes fully galvanic if this capacitive coupling is shorted via the switch. Due to the fact that the conductive chassis surrounds the device closely, the capacitive return path to earth is not significant due to field lines terminating on the chassis and instead of infinity (earth ground). It is like a bi-phasic HBC system due to the fact that the current primarily flows from the signal electrode of the transmitter to the car body and directly to the transmitter ground on the same device without traversing through some capacitive return path. Hence, the return path of the receiver device has little to no bearing on the channel and is not depicted. Higher currents driven through the conductive chassis allow a local potential difference to be detected close to the transmitter; however, it decays strongly as a function of distance through a ladder of impedances.

Figure 2b illustrates an outside-excitation capacitive return path scenario. The received signal is once again represented by Electrode 1 and Electrode 2. However, with both the transmitter and receiver ground being outside of the vehicle (and physically away from the car chassis), a return path is possible via capacitive coupling to some point outside the vehicle (potentially earth ground). Hence, the current is lower than in the inside excitation scenario due to multiple high impedance return path capacitances. However, the signal can be conducted with lower loss for the full extent of the chassis and not receive as much decay as is characteristic of quasistatic electric fields at the rear of the vehicle. This mode is analogous to capacitive return path modes in HBC theory, such as the works of Maity et al.[15], as the loss is flat along the extent of the conductor. Finally, Fig. 2c shows the theoretical diagram for the resonant cavity mode. Unlike the previous modes of communication, the frequency here is significantly higher (>30 MHz), hence an RF generator and wave modeling are necessary. The vehicle consists of an RLC model typical of a cavity resonator, and an EM standing wave pattern is generated inside the vehicle at the resonant frequency as fixed by the car chassis dimensions. The spectrum analyzer and buffer emulating a receiver remain consistent between each of the proposed

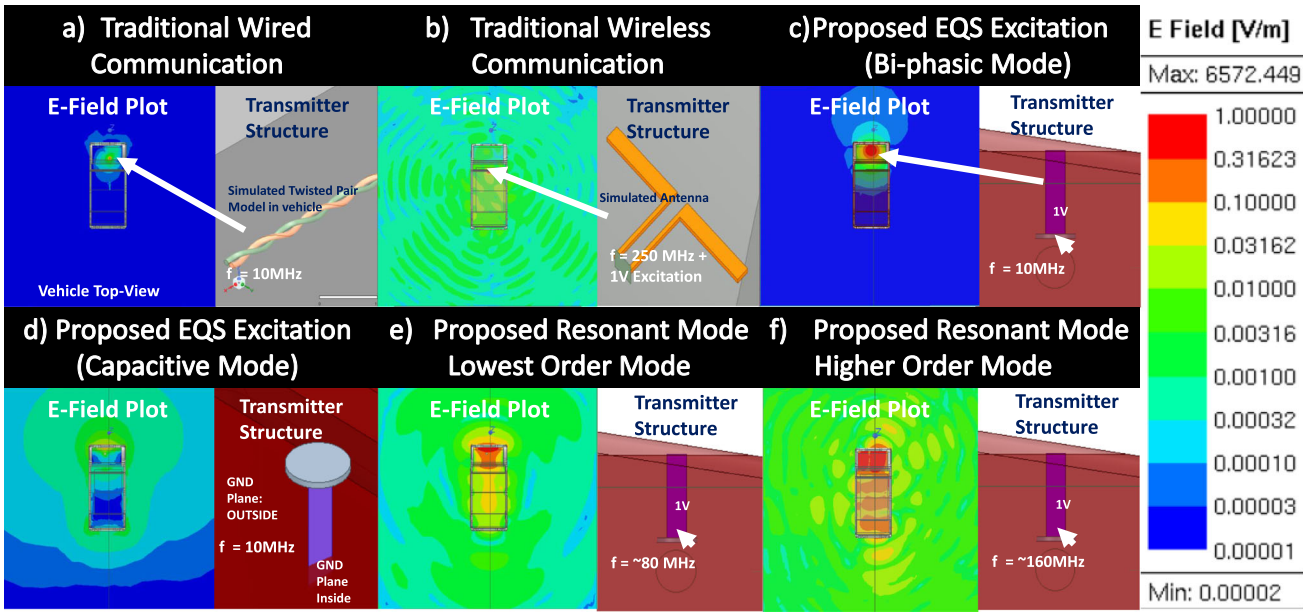

Channel Loss can be computed using: RX Voltage = Effective Coupler Length * Electric Field I .e. .010m x .1 V/m = .001V which is equivalent to 60dB Voltage Loss as the excitation is 1V

Fig. 3 | Electric field magnitude plots comparison for proposed modes. a Traditional twisted pair connection. **b** Wireless radio dipole antenna. **c** Inside capacitive return mode excitation. **d** Outside capacitive return mode excitation. **e** Resonance mode at 82 MHz. **f** Resonance at 166 MHz with mode conversion.

physical communication techniques in simulation and measurement. It is important to note that all the excitation modes are single-wire with a return path formed purely through physical coupling of the ground parasitic of each excitation device.

Electric field simulations on various communication modalities

A set of electric field magnitude plots in Fig. 3 derived from numerical EM simulations highlights the key differences of the proposed modes compared to the current traditional methods from a channel loss and electric field distribution around the vehicle body. The field plots are shown from a top view of the vehicle and solved for a 12 × 12 meter space around the vehicle. Communication channel loss can be estimated by the product of electric field intensity and effective coupler length, or more simply, the device height (i.e., 1 V/m × 0.01m results in 60 dB channel loss in voltage).

Traditional wired and wireless communication. Figure 3a shows the most common intra-vehicle communication medium of today, a twisted pair. The twisted pair is excited by a 1 V excitation between the conductors and confines the signal tightly around the twisted pair with a maximum field intensity of approximately 1 kV/m. Clearly, the twisted pair offers the gold standard in terms of both signal confinement and low signal loss. This will continue to be required to support higher data rate gigabit per second links (i.e., Ethernet) for vehicle applications in autonomous/infotainment. The major drawback of twisted pair is the increasing packaging complexity and logistics. On the other hand, Fig. 3b plots a radiative wireless network. This presents a significant security vulnerability as communications in this frequency region and above radiate in all directions. This enables propagation of EM waves through free space, which can lead to remote hacking or spoofed signals. Even worse, locally, the receiver is only picking up a small aperture of the transmitted signal, as well as losses due to the lossy conductor structure, tight packaging, and lack of line of sight, resulting in poor reliability.

Capacitive return path communication medium. For low data control signals (< 1 Mbps), instead of using an EM wave, a wireless option using the quasi-static frequencies is sufficient for communication (Fig. 3c). This is achieved by coupling an electric field along the car body, similar to a shell or guided medium-based communication. Furthermore, by keeping the ground metal of the receiver inside the vehicle body floating, maximum signal confinement is realized as the conductive vehicle chassis provides shielding from outside hacking. In contrast, it is possible to communicate along the entire chassis if the floating ground of the transmitter device is exposed on the outside of the vehicle at the cost of reduced signal confinement. Figure 3d highlights the field pattern of this scenario. A weak electric field is capacitively coupled onto the surface of the vehicle and dies off within a meter from the vehicle.

Depending on the placement of the ground conductor and channel range requirements, the capacitive return-path based communication modalities can choose to keep the signal completely contained, close, and shorter range (~1 m). The observed phenomenon can be potentially explained by the recent advances in the theory of Bi-Phasic Galvanic communication modality for HBC by Chatterjee et al.[23]. A similar model can also be designed to communicate around the surface of the entire chassis at the cost of increasing attack surface. The channel loss for the capacitive mode is higher for outside excitation at short distances. However, as the distance increases to the rear of the vehicle, outside excitation channel loss stays at a constant value (10 mV/m), whereas the inside excitation mode continues to drop off. The security properties of inside excitation modality are enabled by the EQS technique, as the chassis is able to provide shielding for such low-frequency signals. In other words, there is no significant EM wave component at the right length scale to escape the car chassis.

Vehicle resonant cavity mode simulations. Though capacitive return path excitation provides excellent signal confinement, the channel loss for a 10 cm effective length receiver is still primarily in the 70–80 dB regime. This loss range practically translates to low megabits per second (Mbps) to kilobits per second (kbps) communication links. This numerical analysis can be backed by doing an approximate calculation using Shannon–Hartley theorem.

$$C = BW * \log_2(1 + SNR) \quad (1)$$

C refers to the theoretical channel capacity, SNR is the ratio of signal to noise ratio and BW is the available bandwidth for the communication. EQS

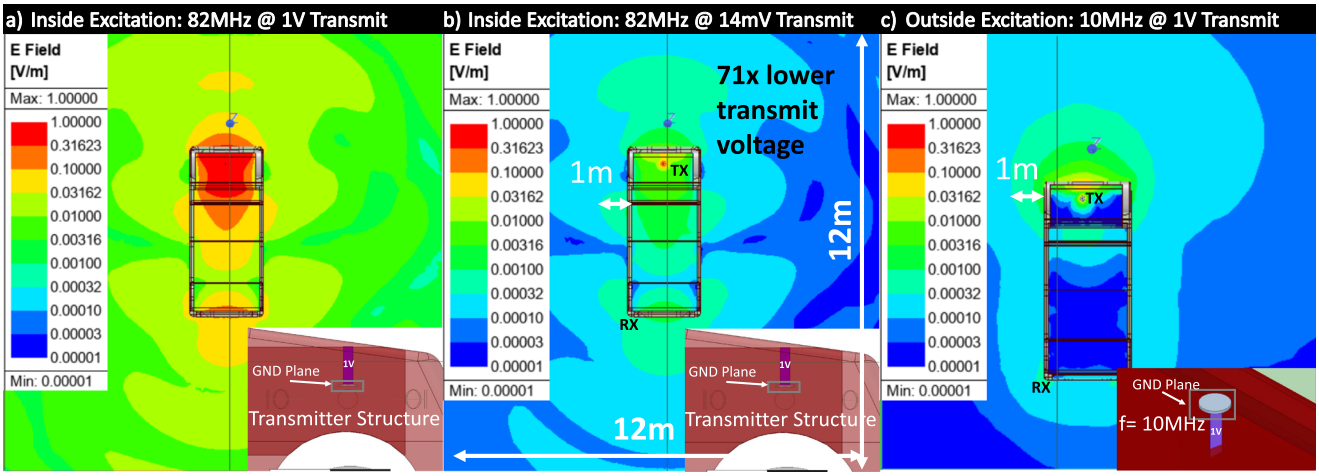

Fig. 4 | Voltage scaling example. Shows electric field plots with (**a**) 1 V excitation at 82 MHz in resonant cavity mode. **b** 14 mV excitation at 82 MHz in resonant cavity mode. **c** 1 V excitation at 10 MHz in electro-quasistatic mode and Ground (GND) planes of various excitation modes.

modes show at worst an 80 dB channel loss (voltage). For a peak voltage transmission of 1 V this approximately equates to −84 dBV of received signal. Practical state-of-the-art voltage has a noise voltage of −94 dBV (or 20 uV_{rms}), resulting in a 10 dB signal-to-noise ratio. The carrier frequency of operation for this communication system is restricted by the large wavelength requirement (to maintain quasistatic properties)—hence bandwidth is typically limited to 5 MHz or lower.

Given these conditions, it is evident that the channel capacity cannot exceed 18 Mbps. In practice, achieving this number is even more unlikely due to communication overhead.

Furthermore, as evident in Fig. 3d, the channel results in virtually no communication possible (10 uV/m E-field intensity represented by color blue) to the rear interior of the vehicle. Hence, the authors propose a different modality of operation in the vehicle by modeling the vehicle chassis as a resonant cavity.

The chassis frame of the vehicle can be approximated as a rectangular cavity resonator. At particular frequencies of resonance, the cavity walls (made out of conductors) allow EM energy to reflect back and forth between them to generate high-intensity standing waves (30–40 dB or 10–100 mV/m scale intensity). Note that the transmitter structure is identical to the capacitive return-path excitation in Fig. 3c, the only difference is the operation frequency. The loss inside the vehicle walls is orders of magnitude higher than that outside of the vehicle as evident in Fig. 3e, f. This low-loss modality enables very efficient communication and a path to 100's of Mbps links in vehicle from a channel capacity standpoint due to having 100× more signal. Furthermore, the resonant cavity mode operates at a significantly higher frequency (~80–160 MHz as opposed to 1–10), which can increase the bandwidth allocation. However, the trade-off is that localized areas may have signal peaks and troughs due to the wave nature of the signal. On the other hand, voltage scaling can be employed to keep the channel nearly as secure as the capacitive return path modes. In Fig. 3, a transmit voltage of 1 V is utilized in all simulations in order to give an initial comparison of the loss. However, in order to achieve signal confinement, voltage can be scaled down to reduce the leakage from the vehicle. For a given receiver channel from the front to the back of the vehicle, resonance modes present 71× lower loss as compared to capacitive return path communication. Hence, much less transmit voltage is needed to operate at iso-receiver data rate. This is important to mitigate the high fields leaking outside of the vehicle in Fig. 3e, f. Figure 4 shows a comparison of the initial 1 V transmit resonance mode (Fig. 4a) alongside a electric field magnitude plot of the same transmitter with 71× lower transmit voltage (Fig. 4b). As compared to the capacitive return path mode in Fig. 4c which uses a 1 V excitation—the loss is the same for the considered channel having a field intensity of ~1 mV/m at the receiver in the rear of the vehicle (labeled RX in the figure). This plot shows that from a physical security standpoint the leakage signature for the cavity resonator model can be equivalent to the capacitive return path modes by trading off data rate.

Capacitive return path transmitter size and geometry considerations

Simulations of the transmitter geometry and position for the capacitive return path are undertaken to understand the potential variations in channel loss. Unlike in radio frequency wireless design, the EQS or near-field regime is heavily dependent on geometry and coupler dimensions. This is due to the fact that the channel is modeled more as a circuit that has a continuous source, rather than medium for which EM waves propagate after a source creates a disturbance. The floating ground of the transmitter device has a significant effect on the respective channel loss. Figure 5a shows simulation channel loss results for a variety of transmitter device areas. The loss increases rapidly once the area of the transmitter ground falls below 100 cm^2. The transmitter variation versus floating ground area is plotted for several different receivers (3, 6, and 7) where the locations of solution is mapped by the rightmost end of the figure.

In addition to transmitter size, it is necessary to correctly model the surrounding environment as the communication modality in capacitive return path mode is near-field. In Fig. 5b, the transmitter and receiver metal disks are in the hood of the vehicle. The engine block modeled with appropriate materials of cast iron or aluminum alloy presents a more accurate model. The yellow curve signifies the loss if the engine block were not modeled, leading to unrealistically optimistic results. The blue curve models the channel with the engine block highlighted in green block on the right-hand side of the figure. Finally the orange curve is the actual measured channel loss as distance increases.

Capacitive return path in-vehicle measurements

The communication channel for in-vehicle capacitive return-path based transceiver was measured as a function of distance in Fig. 6. The measurements were performed with both inside excitation and outside excitation transmitter structures. The signal is excited through the car ground via the negative terminal of the vehicle battery. Figure 6a, shows the measurement setup for the inside excitation structure where the TX is sitting on the car trunk components. Figure 6b highlights the outside excitation measurement setup, where the TX is set atop the glass windshield above the chassis of the vehicle. Figure 6c shows the receiver locations and receiver setup for several locations. Finally, Fig. 6d shows measured channel gain versus distance overlayed upon the simulated losses in HFSS. The result matches the findings in Fig. 3c where the electric field decays as distance radial to the transmitter increases.

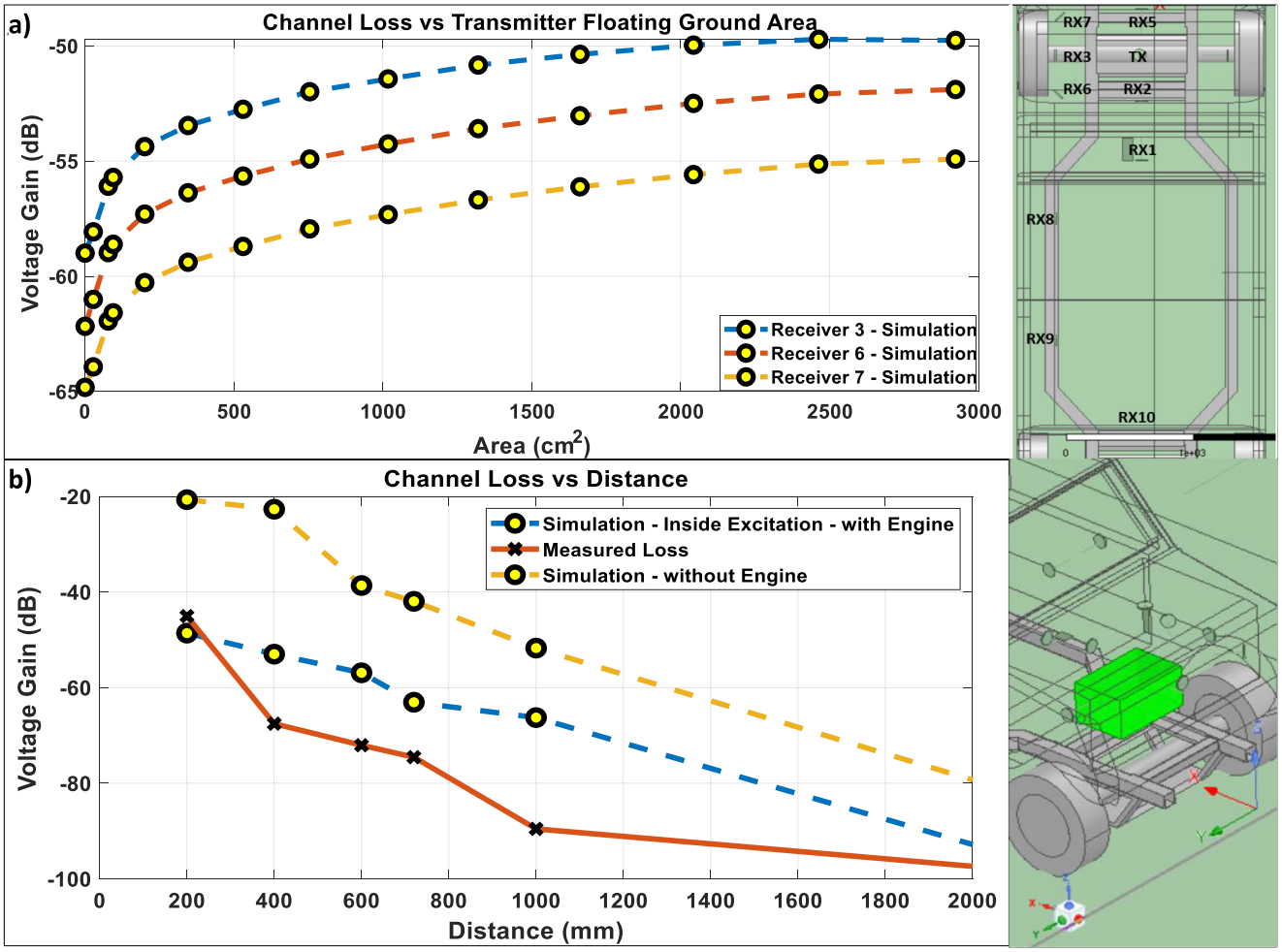

Fig. 5 | Channel response for different-sized devices. Shows the channel response for (**a**) various ground plane sizes on the transmitter, (**b**) with and without the inclusion of a metal engine in the hood.

Furthermore, as distance increases beyond 2.15 meters, the loss saturates to a constant value of approximately 100dB. This loss is consistent with the field patterns simulated in Fig. 3d where the electric field remains constant when channel is across the entire vehicle for the case where the receiver is inside but the transmitter is outside.

Lastly, in Fig. 6e the scenario where the measurement is made with the transmitter and receiver ground plane outside the vehicle. The channel loss is constant ~70–80 dB along the entire vehicle chassis. The measurement confirms the operation modalities and ground plane placement decisions for capacitive return path mode. Security sensitive signals should aim to keep the ground plane as far inside the chassis as possible to take advantage of the loss with distance. For signals that need to traverse the entire vehicle, the communication will most benefit by having the ground plane exposed to the outside of the vehicle at the cost of some leakage.

Safety considerations

The following section discusses the limits on human safety regarding this method of communication and highlights the limit of the applied voltage, though 1 V is the typical excitation used in this study, higher voltages are possible given the following limits are followed.

In the EQS mode, little to no power is propagated through the air as the time-varying magnetic field component of the EM wave is practically nonexistent. The limit of voltage used for human safety would primarily be guided by the AC current safety limits. Generally, the safety limit set by organizations such as the International Electrotechnical Commission (IEC) and International Commission on Non-Ionizing Radiation Protection (ICNIRP) puts the AC current limit at about the ten-milliampere range for 1 MHz. Below this range of AC current, human perception and impact on body is limited, particularly in the MHz regime which cells tend to low pass filter. Though the chance of this communication AC current conducting through the human is highly unlikely, as the impedance from human to ground would be much higher than other paths through the conductive steel alloy chassis. A safety limit of 10 V or 20 V would be wise to stay well under the IEC and ICNIRP limits. Furthermore, since the channel loss of communication is relatively low compared to traditional wireless, the usage of 10 V or 20 V to provide a 20–26 dB SNR boost should be unnecessary in most cases. For the resonant-cavity mode, due to the wave nature of the fields, it is likely that the specific absorption ratio set by the ICNIRP, FCC, and FDA would be the proper guidelines to follow. This is in the range of ~1.6 W/kg of body tissue. However, since the channel loss of the resonant cavity mode is only 20–40 dB, a milliwatt (at least 10x < than the limit) level transmission would be more than sufficient for a sufficient (at least 40 dB) SNR. To determine the limit, one must measure the electric-field as the q-factor will vary with geometry.

Resonant cavity mode channel simulations

Frequency response and lowest order modes. The resonant cavity mode (Fig. 7) is characterized in three categories of locations. These categories are divided based upon the boundary conditions imposed by proximity and size of the surrounding and highly conductive car chassis. These categories are the (i) hood of the vehicle, (ii) main cabin in the center of the vehicle, and (iii) main cabin on the side of vehicle. The hood

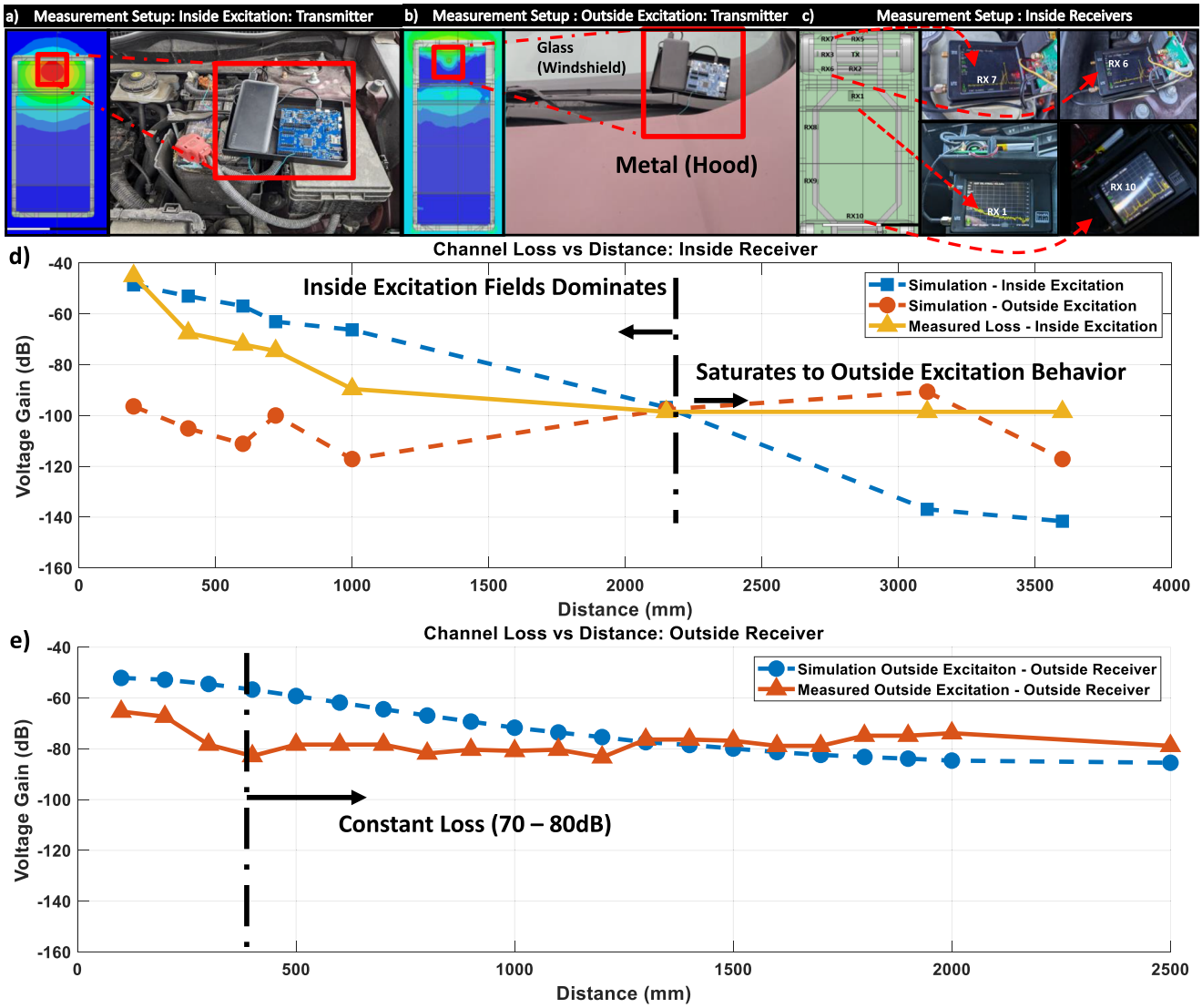

Fig. 6 | Simulated and measured channel response for electro-quasistatic modes. Demonstrates the (**a**) Channel loss inside transmitter setup. **b** Channel loss outside transmitter setup. **c** Receiver setup. **d** Channel loss for receiver inside the car. **e** Channel response for receivers on the surface of the chassis of the car without outside excitation.

of the vehicle is approximated as a rectangular cavity and smaller spatial support than the main cabin and as a result the lowest order mode will be at a higher frequency. The main cabin has two distinct sets of receiver locations—based on whether or not the receiver is located close to the center of the vehicle or close to one of the conducting surfaces. Though the environment has the same spatial support of the main cabin, the receiver coming close to a large conducting surface will create changes in the frequency response. Figure 7a shows the simplified physical picture for the hood of the vehicle. This can be approximated by a rectangular cavity with a PEC boundary on five of the sides. From the side view the lengths are 0.8 and 0.4 meters. From the top view walls the lengths are 0.8 and 2.0 meters. These lengths correspond to the three lengths of the cuboid that makes up the cavity in the hood. Figure 7b shows the channel response over frequency for three different receivers in the hood. Figure 7c, e shows the same simplified physical model as Fig. 7a but with lengths of the cuboid being 1.5 m, 2.0 m, and 3.3 m to represent the main cabin. The main cabin tends to be larger than the hood in nearly all vehicles. The main difference between the two figures is that the receiver in Fig. 7c is in the center of the vehicle where free space is the dominant medium in all directions, whereas Fig. 7e has a large conductive structure (the chassis wall) very close to the receiver in one direction. It can be seen from Fig. 7b that the channel loss is primarily flat with the exception of a peak at 166 MHz as well as troughs located at 76 and 128 MHz. As the frequency varies, the standing waves can fit higher order modes, thus creating many local maximas and minimas in field intensity. The lowest order mode frequency is calculated using the general dispersion equation (2) from Kong's book[24] for rectangular cavity resonator by considering a and b vehicle cavity lengths and p as 0:

$$k_r^2 = \left(\frac{m\pi}{a}\right)^2 + \left(\frac{n\pi}{b}\right)^2 + \left(\frac{p\pi}{c}\right)^2 \tag{2}$$

where

$$k_r^2 = \omega^2 \epsilon \mu \tag{3}$$

If is 2 m × 1 m rectangular cavity resonator is considered, the lowest order mode can be found to be at 167 MHz for free space. Furthermore, all three receiver locations see a peak at this frequency, indicating that the nodes are periodic throughout the structure. Finally, looking at the data presented in Fig. 3f, it can be seen that the field is high intensity through the entire hood of the vehicle. The low-loss channel enabled by these strong standing waves is

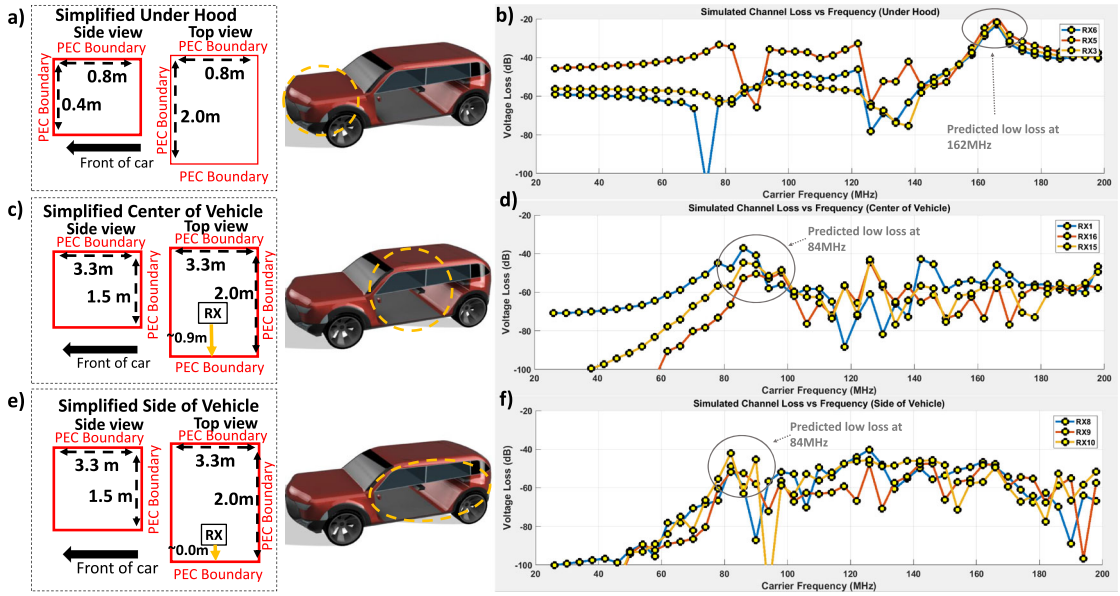

Fig. 7 | Simulated channel loss for resonant cavity modes. Electromagnetic numerical analysis of cavity model (with wall approximated as perfect electrical conductor (PEC)) and channel response for resonant mode in the **a**, **b** hood **c**, **d** center of the main cabin. **e**, **f** Side of the main cabin versus excitation frequency.

significant as it offers paths to high data rates and reliable communication throughout the hood of the vehicle without the need for physical wiring. Though wireless, this communication is not vulnerable to remote attack if transmit voltage scaling is implemented for sensitive signals.

A resonance occurs in the main cabin of the vehicle as evident in Fig. 7c, d. The lowest order peak mode exists primarily at 82 MHz as the peaks of all the receivers have a loss at around 40 dB. This result is in line with theory for rectangular cavity resonators as conductive structure of 4 × 2 meters should roughly have it's lowest order mode at 84 MHz. Furthermore, a peak still occurs at 120 MHz and 166 MHz suggesting that resonant peaks or troughs may exist depending on location of the receiver device. The most interesting implication of this result is that a common frequency of resonance exists between the hood and the main cabin of the vehicle. Inspection of Fig. 3f shows the possibility of mode conversion from the hood (single peak), to a higher mode in the main cabin (3 major peaks) enabling communication between devices in the cabin to the hood. For example, a 166 MHz transmitter in the hood can communicate to the peaks of the higher order mode in the main cabin with 20-40 dB voltage loss.

Lastly, the frequency response behavior of the main cabin resonance is modified when the receiver is brought very close to the wall. As can be seen in Fig. 7e, f, the resonant peaks are less pronounced. The loss in general for non-resonant frequencies are not in the range of 60–80 dB, but rather stay up in the 40–60 dB range. This is hypothesized to be a superposition of standing waves formed in the vehicle at resonance in combination to the capacitive return path communication happening through the side walls of the vehicle. This implies that much higher bandwidth communication is possible if the receiver device is in close proximity with one of the vehicle walls. For example, the loss between 100 MHz to 180 MHz in Fig. 7f shows a consistent voltage loss of around 50dB. When the receiver device is more surrounded by free space, only the resonance frequencies are available for communication and bandwidth is reduced.

Channel loss magnitude in resonant mode. This section discusses the broadband loss characteristics of the channel. The loss in the hood (Fig. 7b) is in the range of 40–60 dB outside of the 166 MHz resonance peak and troughs at 74, 86, 124, and 138 MHz. This low loss is due to the fact that transmit and receive devices are within a meter distance. It can be seen that for greater than 1 meter distance channels in Fig. 7d, the loss in general is about 60–80 dB outside the peaks (20 more than the hood case). This is due to the fact that there is no direct coupling between the devices. For 7f, the additional capacitive coupling makes the loss in the 50–70 dB range.

The peak of the responses in the hood are in the order of 20 dB loss, whereas the peaks in the main cabin are of the magnitude of 40 dB loss. This can be explained by the fact that the devices are further apart and that the quality factor for the hood is better than the main cabin due to less discontinuities or openings. Closer examination of Fig. 4b reveals that the electric field leaks from the window—similar to the operation of a slot cavity antenna. The windows create imperfections in the cavity, which lead to a lower quality factor and additional loss.

Resonant cavity mode channel measurements

Measurements were carried out in the center of the main cabin front and rear seats to characterize the channel loss versus frequency. The measurements plotted in Fig. 8 serve to validate the resonant cavity model proposed in this paper. The channel loss can be seen to be around 20 dB at 62 and 66 MHz for the main cabin. The shift in frequency from the simulation model is the result of non-unity epsilon materials (seats, plastic center console). As the simulations had only air as the medium within the car chassis, the effective wavelength of the EM wave would be higher than predicted, though these are primarily second-order effects. The measurements were carried out in the center of the vehicle to avoid confounding modalities of communication arising from capacitive coupling to the chassis surface and in order to establish clearly the resonant peaks and troughs that exist due to the cavity resonance.

The experiments were performed by exciting the chassis with a frequency sweep from 24 to 200 MHz as shown in Fig. 8a. Voltage channel loss is measured by a voltage coupler and custom buffered front-end as shown in Fig. 8b. The measured response is overlayed with the simulated response from HFSS in 8c. Excitation from the hood led to measured peaks occurring at 62, 66, 98, 118 MHz, and troughs in the region of 140–160 MHz. As higher order modes (200 MHz and above) can potentially lead to significant radiative components, they should be avoided in general for security purposes despite the loss trending back upwards.

Interference measurement on vehicle chassis

Electrical interference from various sources on the vehicle chassis could be a challenge for designers utilizing both EQS and cavity resonant

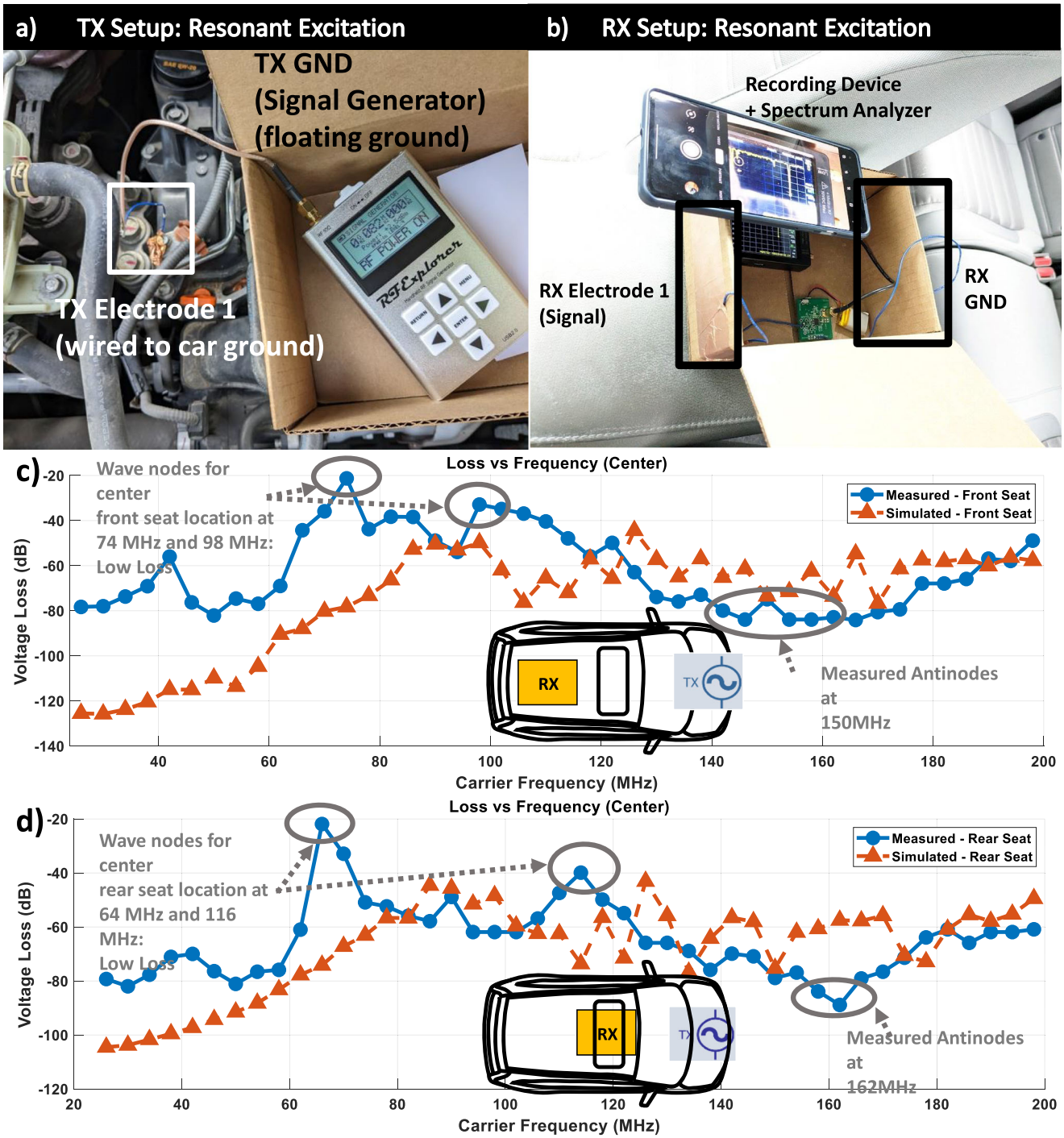

Fig. 8 | Measured and simulated results for two locations in resonant cavity mode. **a** Measurement setup transmitter (TX) for resonant mode measurements. **b** Measurement setup receiver (RX) for resonant mode measurements. **c** Channel response plotted over simulations for front seat and sample location. **d** Channel response plotted over simulations for rear seat and sample location and device ground (GND) locations.

modes of car body communication. Hence, a measurement of the interference that the vehicle picks up is critical to the formulation and feasibility of this system. The interference measured in-vehicle (Fig. 9) utilizing a high-impedance buffer from 250 kHz to 250 MHz is plotted as follows. The key area of interferences are due to FM radio bands. The low frequency interference is from the vehicle electronics when the engine is on. However, the maximum amplitude of non-common grounded interference is still in the hundreds of micro-volts on the chassis, which can easily be overcome with the low loss of the direct excitation of a EQS or Resonant Cavity transmitter.

Performance impact of open vehicle doors and hood

The following section analyzes the impact of changing vehicle chassis geometry on the performance of the proposed communication modes. These experiments ensure communication is still feasible when the doors of the vehicle are open or if vehicle geometry variations due to design differences, temporary damage, and other factors. A study is conducted to determine the variation in channel due to the shift in geometry.

The primary focus of the study focuses on the most common case, when the doors of the vehicle are removed as illustrated in Fig. 10a, b. The effective capacitance to model the car chassis remains remarkably similar with and

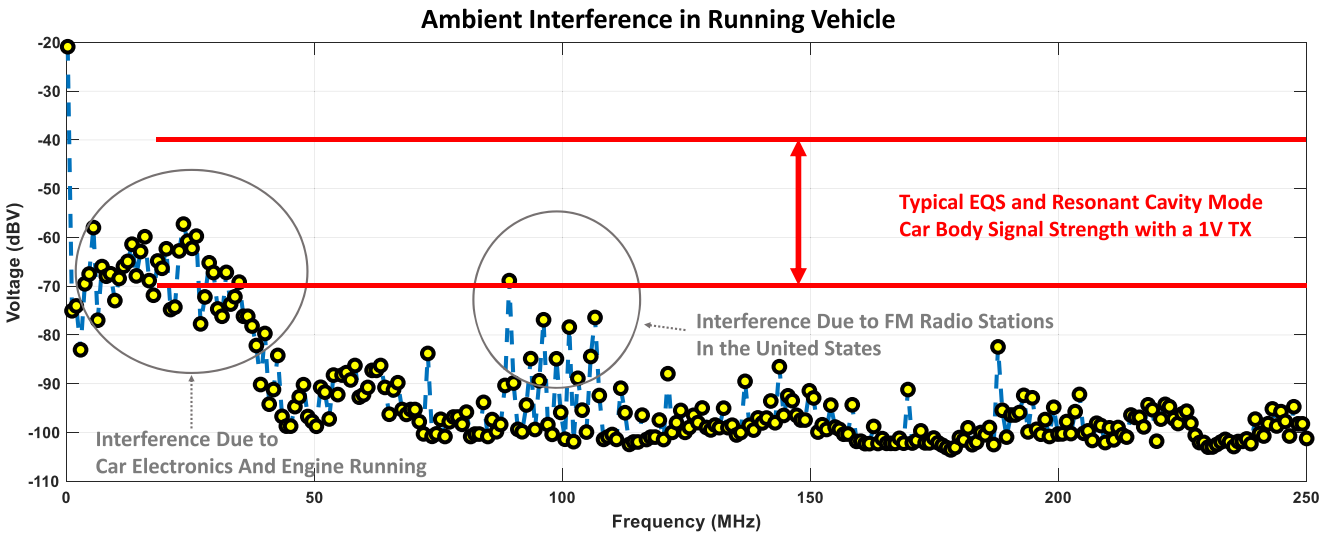

Fig. 9 | In-vehicle interference measurements. Measurement of ambient interference on a running vehicle and annotation of several key sources and typical range of Electro-Quasistatic (EQS) signals overlayed.

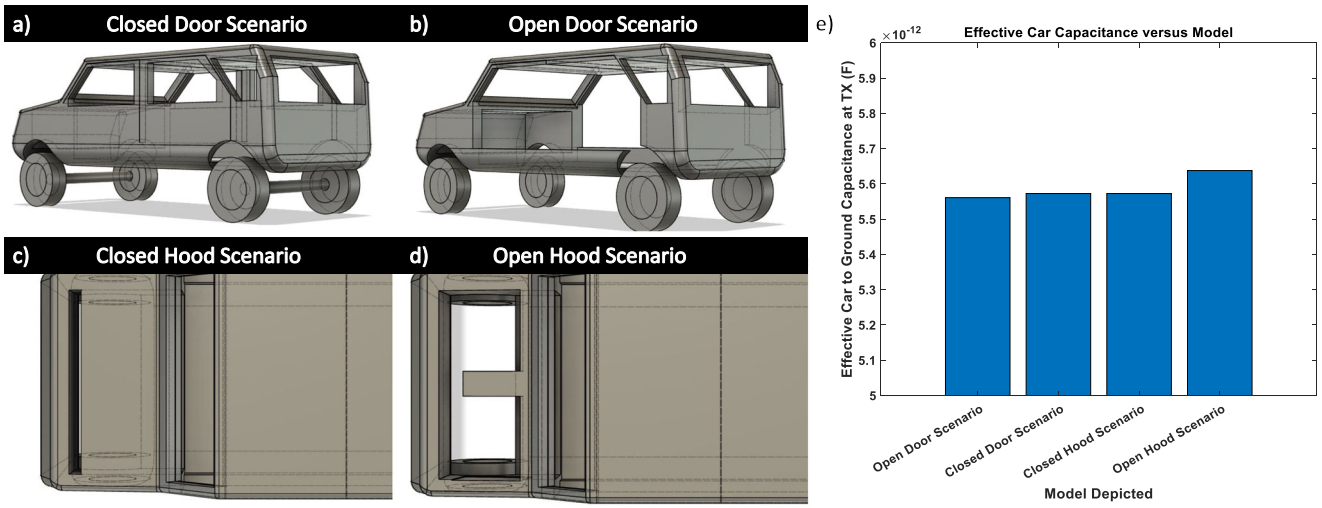

Fig. 10 | Capacitance model variation due to open car door and hood. a illustrates the model used in simulations for the closed door scenario. **b** the model of the open door scenario where the vehicle doors are removed. **c** Model that illustrates the hood of the vehicle in simulation where the hood is closed. **d** where the hood is open. **e** Highlights the capacitance versus different models presented previously in the figure.

without doors as seen in Fig. 10e. The capacitance remains very similar at around five picofarads typically despite the doors being removed from the simulation model. Hence, there is no expected change in the electro-quasi static channel from missing doors from EM simulation.

Similarly, Fig. 10c, d, analyzes two identical models with and without the hood removed, and again the capacitance can be observed to be relatively constant between 5.5 pF to 5.7 pF seen in Fig. 10e.

Furthermore, a study of the resonant cavity mode is performed with the utilization of EM simulations. Figure 11a illustrates the model used in the closed door model simulation. In contrast, 11b shows the model used in the open door simulation. Figure 11c, d show the electric field magnitude as a function of position. Finally, Fig. 11e shows that the channel and frequency locations of resonance and anti-resonance remains consistent to the first order between the two models with slight deviations in frequency and amplitude.

Conclusion

This paper investigates novel, physically secure non-radiative wireless communication methods for automotive bodies, distinct from conventional wired and wireless communication technologies. These communication modes include 1) EQS low frequency modes 2) Resonant Cavity mode. These communication modes provide new ways for devices within a vehicle to physically communicate without the need for traditional twisted pairs. This enables those wired channels to be reserved for high data rate autonomous driving and video data applications. Resonant cavity mode, in particular, can be implemented to give a communication link that is wireless but greatly exceeds the capability of traditional radio frequency techniques while having unique security features. Overall, the studies show great promise for near-field and resonant techniques that take advantage of the fixed and conductive automotive medium. This technology still requires further study in both the area of channel modeling and application demonstrations in order to realize its full potential. It has the potential to augment or even reshape the physical layer network of vehicles in the modern era in the future.

Methods

ANSYS HFSS simulation setup

The simulations for the electric field plots were solved in ANSYS HFSS. Figure 12a shows the vehicle model of dimensions $4 \times 2.7 \times 1.8$ meters was

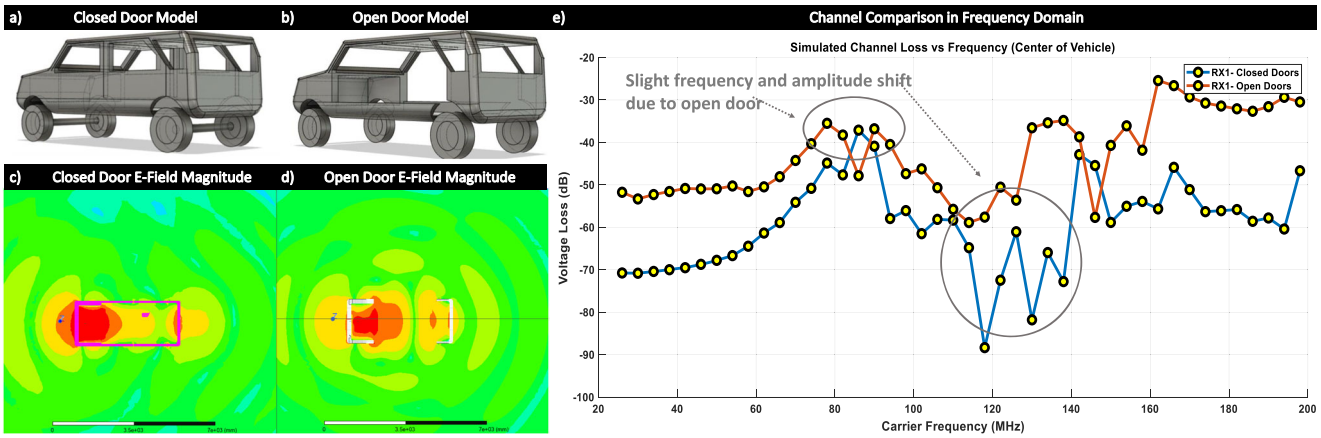

Fig. 11 | Resonant car channel variation due to open door. a Illustrates the model used in simulations for the closed door scenario. **b** The model of the open door scenario where the vehicle doors are removed. **c** The electric field magnitude plot for a closed door model at resonance. **d** The electric field magnitude plot for a open door model at resonance. **e** Voltage channel loss versus frequency for open versus closed door.

modeled for the simulation which is available upon request from the authors. The vehicle main cabin, wheels and axle are assigned the material of steel and tires are assigned rubber (frequency dependent epsilon and sigma). A finite element boundary integral condition is imposed around the vehicle, and empty space is filled with air. This is used instead of radiation boundary condition as it yields more accurate numerical solution when solution space is constrained relative to wavelength (very low frequency operation). Figure 12b shows the transmitter and receiver setups in detail. The transmitters and receivers are aluminum cylinders of radius 50 mm and height of 10mm. These lengths were chosen due to the spatial consideration of a typical ECU and remain constant for all the studies except the one that studies TRx ground plane. A voltage excitation is placed upon the rectangle highlighted in blue, representing an ideal voltage source (Fig. 12b).

A line integral calculation is used to compute the received voltage for all reported data, assuming an effective receiver length of 10 mm on the incident electric field.

Voltage mode and channel loss in capacitive-dominated systems

The authors of the paper primarily use voltage as the metric for channel loss. For near-field (or quasi-static systems), it is possible to use voltage as the sensed quantity rather than power, as the wavelength is significantly larger than the length scale of the object, rendering localized variations of current and voltage negligible.

The main motivation for voltage sensing or voltage mode systems is that it enables implementations to use high impedance terminations. High-impedance termination enables for lower loss at low frequencies as the physical return path capacitances for floating ground devices prevent significant current from flowing in the system and hence poor power-mode based communications. A simple numerical example demonstrates this effect. From theory previously developed for the human body[16], the self-capacitance is the dominant component of the return path capacitance. For the devices of this study and the geometry of disk, the self-capacitance is approximately 5 pF as the equation for self-capacitance of a disk is

$$C_{disk} = 8\epsilon r \tag{4}$$

where r is the radius and ϵ is the dielectric permittivity of free space. Hence, the impedance is ~3 kΩ at 10 MHz. As a result, a typical 50 ohm receiver will have much higher communication losses using power than a receiver with high impedance termination as the parasitic impedance comes in series. This is a deviation from common RF systems where carrier frequency is very high and the communication is not near-field.

To illustrate this point more clearly, the authors have used an approximate circuit model of the physical setup in Fig. 13. Figure 13a is the complete circuit picture with all physical nodes in place, a transmitter with

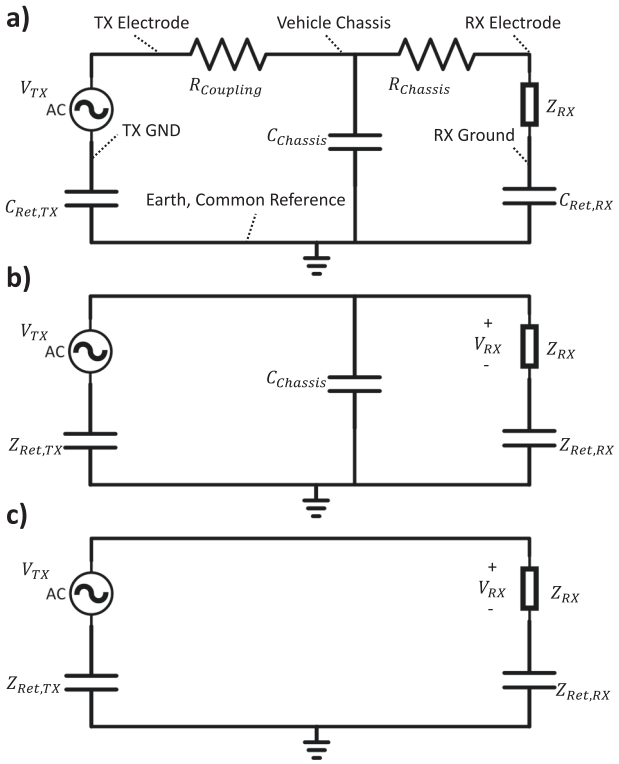

Fig. 12 | Setup for electromagnetic simulations in ANSYS HFSS. a Numerical electromagnetic simulation car model with boundary condition setup. **b** Numerical electromagnetic simulation transmitter excitation model setup within the car alongside engine block model. **c** Final simplified Electro-Quasistatic model without forward path resistances or high vehicle body to earth capacitance.

voltage (V_{TX}) with a floating ground is exciting the vehicle through a $R_{coupling}$ which includes the source resistance of the transmitter. The vehicle chassis presents a capacitance to earth ($C_{chassis}$) as well as a small resistance through the steel frame ($R_{chassis}$). The receiver picks up a signal across it's termination (Z_{RX}) relative the receiver ground. The grounds of the transmitter and receiver devices couple to the earth or some reference in the environment through $C_{Ret,TX}$ and $C_{Ret,RX}$. In Fig. 13b, simplifications are made as the resistance through a large car steel frame and the electrode contact in the single ohm range are approximated as 0. Finally, since the car area is so much larger than the ECU devices, $C_{chassis}$ should be large, and the impedance will come in parallel with $Z_{RX} + Z_{Ret,RX}$ and hence can be

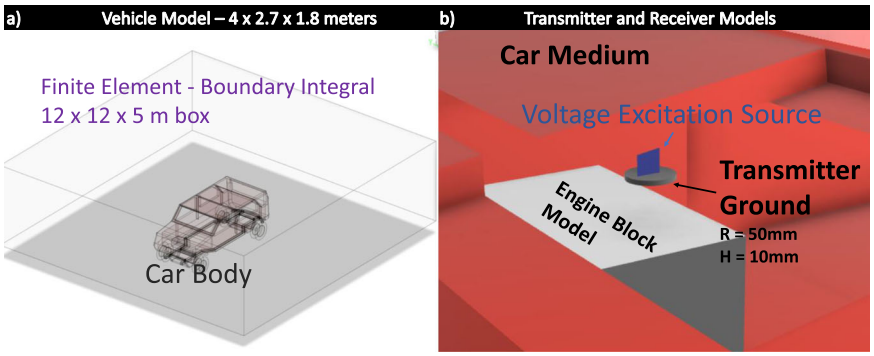

Fig. 13 | Simulation Setup. a Complete electro-quasistatic circuit model without any physical simplifications. **b** Simplified electro-quasistatic model without forward path resistances. **c** Final simplified Electro-Quasistatic model without forward path resistances or high vehicle body to earth capacitance.

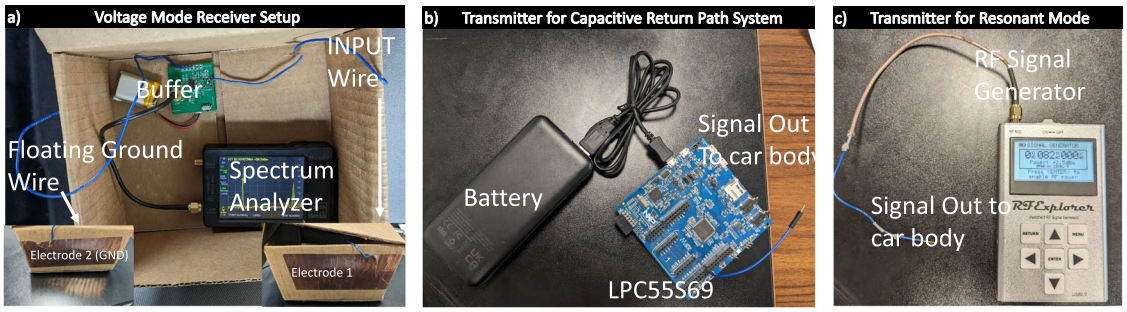

Fig. 14 | Setup for voltage channel measurements in experiments. a Receiver setup for voltage mode receiver for all measurements. **b** Transmitter setup for capacitive return path system measurements (1 MHz excitation). **c** Transmitter setup for resonant cavity mode measurements (24 MHz–1 GHz).

approximated as an open circuit. These approximations are even more applicable as the human body is not as conductive as the steel or aluminum typically used in the car chassis.

Finally, it is possible to derive for channel loss given by

$$\frac{V_{TX}}{V_{RX}} = \frac{Z_{RX}}{Z_{RX} + Z_{Ret,TX} + Z_{Ret,RX}} \tag{5}$$

which shows that maximizing Z_{RX} reduces the loss. Unfortunately, there is typically a shunt path coupling between the receiver ground with the chassis, which can cause a reduction in Z_{RX}, this effect is more pronounced for the vehicle as opposed to the human body as the chassis is significantly more conductive.

Measurement setup for EQS capacitive return path communication

The transmitter for EQS Capacitive Return Path measurements uses the LPC55S69 microcontroller EVK to send a 3.3 V excitation at 10 MHz on the vehicle chassis from the hood illustrated Fig. 14b. The receiver channel is measured utilizing a custom buffer front end that contains a Texas Instruments OPA2836 op-amp configured in unity gain configuration and powered by a lithium polymer battery as shown in Fig. 14a. This signal is then input to a commercially available TinySA Spectrum Analyzer via SMA coaxial cable. Due to the fact most spectrum analyzers commercially available have a 50 ohm termination, the unity-gain buffer enables a high impedance termination while measuring the voltage at the buffer input, which is necessary for EQS-based voltage system measurements. The sensed voltage is calculated from the power measurement read off from the spectrum analyzer and calibrated for device error against a known voltage source. The receiver also contains two 5×15 cm copper electrodes, which have the approximate area of the conductors used in the simulations, as capacitance is directly proportional to coupler area. The peak-to-peak voltage from this calculation is then utilized to calculate channel loss, given the excitation voltage of 3.3 V.

Measurement setup for resonant cavity mode

The transmitter used is the commercially available SEEED Technologies RF Explorer Signal Generator (P.N. 114990081), which generates test RF signals from 23.4 MHz to 6 GHz (Fig. 14c). The vehicle is excited from the chassis in the hood. The same TinySA voltage receiver setup used for capacitive characterization is utilized to characterize the electric field intensity. The voltage loss is calculated based on the measured transmit voltage from the RF power generator via a calibration test.

Data availability

The data that support the plots within this paper and other findings of this study are available from the corresponding author upon reasonable request.

Code availability

Custom codes used to process the data are available from the corresponding author upon reasonable request.

Received: 25 October 2023; Accepted: 31 March 2025;
Published online: 21 May 2025

References

1. ISO. ISO 17987-7:2016. https://www.iso.org/standard/61229.html. (2016).
2. Tuohy, S. et al. Intra-vehicle networks: a review. *IEEE Trans. Intell. Transp. Syst.* **16**, 534–545 (2015).
3. Lu, N., Cheng, N., Zhang, N., Shen, X. & Mark, J. W. Connected vehicles: solutions and challenges. *IEEE Internet Things J.* **1**, 289–299 (2014).
4. Zeng, W., Khalid, M. A. S. & Chowdhury, S. In-vehicle networks outlook: achievements and challenges. *IEEE Commun. Surv. Tutor.* **18**, 1552–1571 (2016).
5. Moghimi, A. R., Tsai, H.-M., Saraydar, C. U. & Tonguz, O. K. Characterizing intra-car wireless channels. *IEEE Trans. Veh. Technol.* **58**, 5299–5305 (2009).
6. Tsai, H.-M. et al. Feasibility of in-car wireless sensor networks: a statistical evaluation. In *2007 4th Annual IEEE Communications*

Society Conference on Sensor, Mesh and Ad Hoc Communications and Networks, 101–111 (2007).
7. Zhang, T., Antunes, H. & Aggarwal, S. Defending connected vehicles against malware: challenges and a solution framework. *IEEE Internet Things J.* **1**, 10–21 (2014).
8. Al-Jarrah, O. Y., Maple, C., Dianati, M., Oxtoby, D. & Mouzakitis, A. Intrusion detection systems for intra-vehicle networks: a review. *IEEE Access* **7**, 21266–21289 (2019).
9. Fowler, B. Jeep hackers back at Black Hat with new and scarier method. https://phys.org/news/2016-08-jeep-hackers-black-hat-scarier.html.
10. ISO. ISO 11898-2:2016. https://www.iso.org/standard/67244.html. (2016).
11. Makowitz, R. & Temple, C. Flexray—a communication network for automotive control systems. In *2006 IEEE International Workshop on Factory Communication Systems*, 207–212 (2006).
12. MOST Cooperation: Specifications. https://www.mostcooperation.com/specifications/.
13. IEEE standard for ethernet amendment 1: physical layer specifications and management parameters for 100 Mb/s operation over a single balanced twisted pair cable (100BASE-T1). In *IEEE Std 802.3bw-2015*, 1–88 (2016).
14. Zimmerman, T. G. Personal area networks: near-field intrabody communication. *IBM Syst. J.* **35**, 609–617 (1996).
15. Maity, S. et al. Bio-physical modeling, characterization, and optimization of electro-quasistatic human body communication. *IEEE Trans. Biomed. Eng.* **66**, 1791–1802 (2019).
16. Nath, M., Maity, S. & Sen, S. Toward understanding the return path capacitance in capacitive human body communication. *IEEE Trans. Circuits Syst. II: Express Briefs* **67**, 1879–1883 (2020).
17. Sen, S. & Maity, S. Communication device and method of making the same https://patents.google.com/patent/US20210258080A1/en. (2021).
18. Das, D., Maity, S., Chatterjee, B. & Sen, S. Enabling covert body area network using electro-quasistatic human body communication. *Sci. Rep.* **9**, 4160 (2019).
19. Varga, V., Vakulya, G., Sample, A. & Gross, T. R. Enabling interactive infrastructure with body channel communication. *Proc. ACM Interact. Mob. Wearable Ubiquitous Technol.* **1**, 1–29 (2018).
20. Varga, V., Wyss, M., Vakulya, G., Sample, A. & Gross, T. R. Designing groundless body channel communication systems: performance and implications. In *Proceedings of the 31st Annual ACM Symposium on User Interface Software and Technology*, UIST '**18**, 683–695 (Association for Computing Machinery, New York, NY, USA, 2018).
21. Gerla, M. & Kleinrock, L. Vehicular networks and the future of the mobile internet. *Comput. Netw.* **55**, 457–469 (2011).
22. Kenney, J. B. Dedicated short-range communications (DSRC) standards in the United States. *Proc. IEEE* **99**, 1162–1182 (2011).
23. Chatterjee, B. et al. Biphasic quasistatic brain communication for energy-efficient wireless neural implants. *Nat. Electronics* **6**, 1–14 (2023). https://www.nature.com/articles/s41928-023-01000-3.
24. Kong, J. A. Electromagnetic wave theory. In *Electromagnetic Wave Theory*, 1st edn., 165–170 (John Wiley & Sons, Inc., 1975).

Acknowledgements

This work was supported by Quasistatics, Inc. DBA Ixana—Grant 40003567, Account F.00127126.02.036. The authors would like to thank Mayukh Nath, Ph.D. from Sparclab, for his valuable inputs during the development of the theory of vehicle as a resonant cavity device.

Author contributions

D.Y. and S.S. conceived the idea. D.Y and S.S. conducted the theoretical analysis, D.Y conducted the numerical simulations and experiments. Both authors analyzed the results and reviewed the manuscript.

Competing interests

The authors declare no competing interests.

Additional information

Correspondence and requests for materials should be addressed to Shreyas Sen.

Peer review information *Communications Engineering* thanks Ahmed Eltawil and Jingna Mao for their contribution to the peer review of this work. Primary Handling Editors: [Mengying Su and Rosamund Daw].

Reprints and permissions information is available at http://www.nature.com/reprints

Publisher's note Springer Nature remains neutral with regard to jurisdictional claims in published maps and institutional affiliations.

Open Access This article is licensed under a Creative Commons Attribution-NonCommercial-NoDerivatives 4.0 International License, which permits any non-commercial use, sharing, distribution and reproduction in any medium or format, as long as you give appropriate credit to the original author(s) and the source, provide a link to the Creative Commons licence, and indicate if you modified the licensed material. You do not have permission under this licence to share adapted material derived from this article or parts of it. The images or other third party material in this article are included in the article's Creative Commons licence, unless indicated otherwise in a credit line to the material. If material is not included in the article's Creative Commons licence and your intended use is not permitted by statutory regulation or exceeds the permitted use, you will need to obtain permission directly from the copyright holder. To view a copy of this licence, visit http://creativecommons.org/licenses/by-nc-nd/4.0/.

© The Author(s) 2025